CHANNELS
2020, VOL. 14, NO. 1, 362–379
https://doi.org/10.1080/19336950.2020.1829842

Taylor & Francis
Taylor & Francis Group

REVIEW

OPEN ACCESS Check for updates

$Ca_v2.3$ channel function and Zn^{2+}-induced modulation: potential mechanisms and (patho)physiological relevance

Felix Neumaier [a,b], Toni Schneider [c], and Walid Albanna [d]

[a]Forschungszentrum Jülich GmbH, Institute of Neuroscience and Medicine, Nuclear Chemistry (INM-5), Jülich, Germany; [b]University of Cologne, Faculty of Medicine and University Hospital Cologne, Institute of Radiochemistry and Experimental Molecular Imaging, Cologne, Germany; [c]Institute of Neurophysiology, Faculty of Medicine and University Hospital Cologne, Cologne, Germany; [d]Department of Neurosurgery, RWTH Aachen University, Aachen, Germany

ABSTRACT

Voltage-gated calcium channels (VGCCs) are critical for Ca^{2+} influx into all types of excitable cells, but their exact function is still poorly understood. Recent reconstruction of homology models for all human VGCCs at atomic resolution provides the opportunity for a structure-based discussion of VGCC function and novel insights into the mechanisms underlying Ca^{2+} selective flux through these channels. In the present review, we use these data as a basis to examine the structure, function, and Zn^{2+}-induced modulation of $Ca_v2.3$ VGCCs, which mediate native R-type currents and belong to the most enigmatic members of the family. Their unique sensitivity to Zn^{2+} and the existence of multiple mechanisms of Zn^{2+} action strongly argue for a role of these channels in the modulatory action of endogenous loosely bound Zn^{2+}, pools of which have been detected in a number of neuronal, endocrine, and reproductive tissues. Following a description of the different mechanisms by which Zn^{2+} has been shown or is thought to alter the function of these channels, we discuss their potential (patho)physiological relevance, taking into account what is known about the magnitude and function of extracellular Zn^{2+} signals in different tissues. While still far from complete, the picture that emerges is one where $Ca_v2.3$ channel expression parallels the occurrence of loosely bound Zn^{2+} pools in different tissues and where these channels may serve to translate physiological Zn^{2+} signals into changes of electrical activity and/or intracellular Ca^{2+} levels.

ARTICLE HISTORY
Received 17 September 2020
Revised 23 September 2020
Accepted 24 September 2020

KEYWORDS
Voltage-gated calcium channels; endogenous loosely-bound Zn^{2+}; vesicular Zn^{2+}; synaptic Zn^{2+}; pharmacoresistant R-type Ca^{2+} currents; metalloneurochemistry; ionic pore block; allosteric modulation; selective permeation; ca^{2+} channel structure and function

Introduction

Zn^{2+}, the second most abundant trace metal ion in mammals, is a well-known component of many proteins and co-factor in various enzymes [1,2]. Apart from its structural and catalytic functions, Zn^{2+} has been identified as a modulator of neuronal transmission, neuroendocrine function, and other processes [2–5]. These modulatory actions depend on a small pool of endogenous Zn^{2+} that is almost exclusively located in synaptic or secretory vesicles and not tightly bound by zinc metalloproteins, so that it remains thermodynamically and kinetically accessible. Spontaneous and activity-dependent release of vesicular Zn^{2+} have been convincingly demonstrated in a number of tissues [3,4,6], although the exact magnitude of the resulting Zn^{2+} signals and their targets remain a matter of debate. $Ca_v2.3$ channels belong to the group of high voltage-activated (HVA) voltage-gated calcium channels (VGCCs) and are responsible for Ca^{2+} influx into neuronal, neuroendocrine and other cells. They mediate the major portion of native R-type currents, which are characterized by their resistance to most organic Ca^{2+} channel antagonists and sensitivity to the tarantula toxin SNX-482 [7–9]. In addition, $Ca_v2.3$ channels are among the most sensitive molecular targets of Zn^{2+} currently known and expressed in many Zn^{2+}-enriched tissues, suggesting that they are involved in the modulatory actions of endogenous Zn^{2+}. The aim of the present article is to provide a concise overview of $Ca_v2.3$ channel structure and function, with a special focus on Zn^{2+}-induced modulation and its potential (patho) physiological relevance. To this end, section two will resort to a recently published homology model of human $Ca_v2.3$ channels at atomic resolution [10] to illustrate their structure and discuss different mechanisms by which Zn^{2+} has been shown or is thought to

CONTACT Felix Neumaier felix@neumaier-net.de Forschungszentrum Jülich GmbH, Institute of Neuroscience and Medicine, Nuclear Chemistry (INM-5), Wilhelm-Johnen-Str., Jülich 52428, Germany

alter Ca^{2+} influx through these channels. The third section will briefly summarize current knowledge about their expression and role in neuronal, endocrine, and reproductive tissues, while the fourth section will consider the effects of Zn^{2+} in terms of their potential (patho)physiological relevance, taking into account what is known about extracellular Zn^{2+} signals in these tissues.

$Ca_v2.3$ channel structure, function and Zn^{2+} induced modulation

Membrane topology

Like other HVA VGCCs, $Ca_v2.3$ channels in native membranes form multi-subunit complexes made up of a pore-forming $Ca_v\alpha_1$-subunit, one of several cytoplasmic $Ca_v\beta$-subunits and one of several extracellular $Ca_v\alpha_2\delta$-subunits. The $Ca_v\alpha_1$-subunit is a pseudotetrameric protein with four homologous repeats (I–IV), which are composed of six membrane-spanning helical segments (S1-S6) [11] (Figure 1(a, b). Four of the segments (S1-S4) in each repeat form a voltage-sensor module (VSM), while the remaining two segments (S5-S6) from all repeats make up most of the pore domain (PD) and the intracellular activation gate (Figure 1c). The extracellular pore mouth and the selectivity filter are formed by reentrant pore loops (p-loops) between segments S5 and S6 (Figure 1c), which partly fold back into the single-file region of the pore [12,13] (Figure 1d). The three inter-domain linkers and other cytoplasmic parts of the channel (not shown in Figure 1) are involved in inactivation, the association of auxiliary $Ca_v\beta$-subunits, and intracellular modulation [14].

Voltage-dependent gating and gating modulation

The exact processes involved in Ca^{2+} channel gating are still incompletely understood, but its

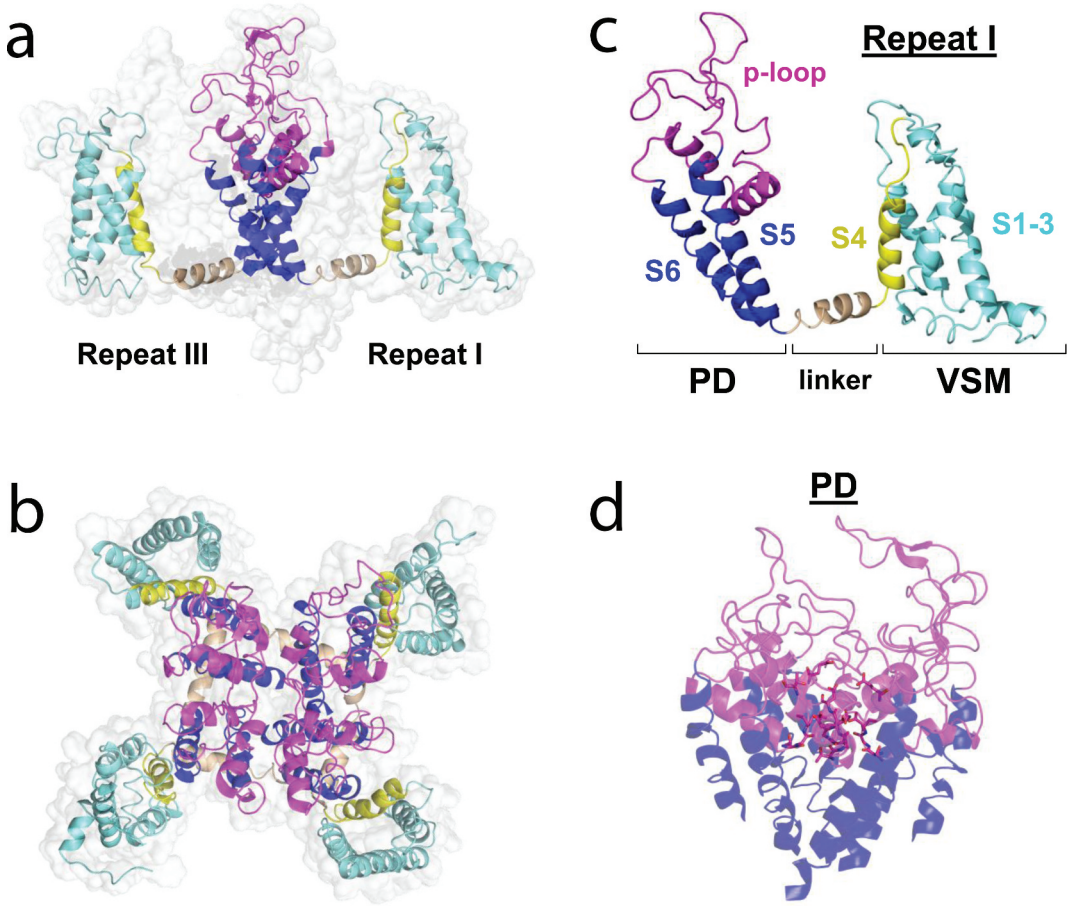

Figure 1. Structure of human $Ca_v2.3$ voltage-gated calcium channels.

Cartoon representation of a homology model of human $Ca_v2.3$ channels at atomic resolution. Depicted are (**a**) *side view showing two of the four repeats*, (**b**) *top view showing all four repeats*, (**c**) *side view of repeat I with the different functional domains indicated below, and* (**d**) *side view of the pore-forming domains from all four repeats* [10].

coupling to the membrane potential is thought to depend on the same mechanism as in all voltage-gated ion channels. At resting membrane potentials, the local electric field drags the positively charged S4 segments toward the cell's interior and parts of the S5 and S6 segments occlude the conduction pathway. Depolarization results in outward movement of the S4 segments through the electric field, relocation of the S5 and S6 segments and formation of a crevice, which ions can traverse [15,16]. In electrophysiological recordings, these charge-moving conformational changes are reflected in a steep change of channel open probability over a narrow range of membrane potentials and, after block of ion conduction, as measurable gating currents. Co-expression of auxiliary subunits affects the voltage-dependence and kinetics of ionic but not gating currents, suggesting that they alter the coupling between voltage-sensor movement and channel opening [17–20]. In voltage-gated sodium channels, activation of the VSMs in repeats I–III is coupled to channel opening [21], while activation of the VSM in repeat IV gives rise to a short-lived second open state that precedes inactivation [22–24]. Interestingly, these findings are already implicit in the classical Hodgkin and Huxley model with its three activation and one inactivation particles for the sodium conductance [25,26]. Less is known about the situation in VGCCs, which have most commonly been described by a combination of two or three activation and one or more inactivation particles [27–30]. However, optical tracking of $Ca_v1.2$ channel voltage-sensor movement in combination with kinetic modeling revealed that, depending on the exact subunit composition, activation of two or three VSMs may indeed be sufficient for Ca^{2+} channel opening [31–33], which is reinforced by mutational studies [34,35], evidence for the existence of multiple open states [36–38] and a slow component of charge movement in gating current recordings [17,39,40]. Also, when a large set of $Ca_v2.3+\beta_3$ channel ionic and gating currents recorded in our lab was fitted with obligatory models in which activation of 2–4 VSMs was required for channel opening, a good agreement between experimental and modeled currents was only obtained when just two VSMs are coupled to channel opening [40]. In this context, it is interesting to note that structural determinants in two of the four repeats (III and IV) have been shown to be a prerequisite for SNX-482-induced shifts in $Ca_v2.3$ channel gating [9], suggesting that activation of the VSMs in these repeats could either be directly coupled to channel opening or associated with a stabilization of the open state.

Moderate acidification or low micromolar concentrations of Zn^{2+} and certain other trace metal ions potently suppress native and cloned $Ca_v2.3$ channels (Figure 2a) by shifting voltage-dependent gating to more depolarized test potentials (Figure 2b), and produce a dramatic slowing of macroscopic activation (Figure 2c) that cannot be accounted for by the shift in channel voltage-dependence alone [40–49]. This unique trace metal sensitivity has been convincingly linked to three non-conserved histidine residues (His_{111}, His_{179} & His_{183}) on the repeat I VSM (Figure 2d), which could form a high-affinity trace metal-binding site. Replacement of these residues by site-directed mutagenesis significantly reduces the gating effects of Zn^{2+}, Cu^{2+}, Ni^{2+} and protons but does not prevent them completely [42,43,47]. In addition, a detailed analysis of the Zn^{2+} concentration-dependence for shift and slowing performed in our lab revealed two separable components with vastly different affinities (Figure 2e), which could also be distinguished based on their sensitivity to histidine modification with DEPC [40]. High-affinity shift and slowing were sensitive to DEPC pre-treatment (Figures 2c & e), could be well described by a common IC_{50} value (2.3–4.4 μM with 2–4 mM free Ca^{2+}) and reproduced with the simplified model mentioned above by assuming that Zn^{2+} binding to a single site leads to electrostatic modification and mechanical slowing of one of the VSMs. Low-affinity shift (IC_{50} > 500 μM) and slowing (IC_{50} ~ 100–200 μM), on the other hand, were insensitive to histidine modification (Figure 2e), suggesting that they are not related to the putative trace metal-binding site in repeat I. However, the low-affinity slowing appeared to be correlated with Zn^{2+} effects on permeation, which will be discussed below in the context of ionic block (see section 2.3). More importantly, we also found that, depending on the holding potential (HP), high-affinity binding could either inhibit or stimulate Ca^{2+} influx through

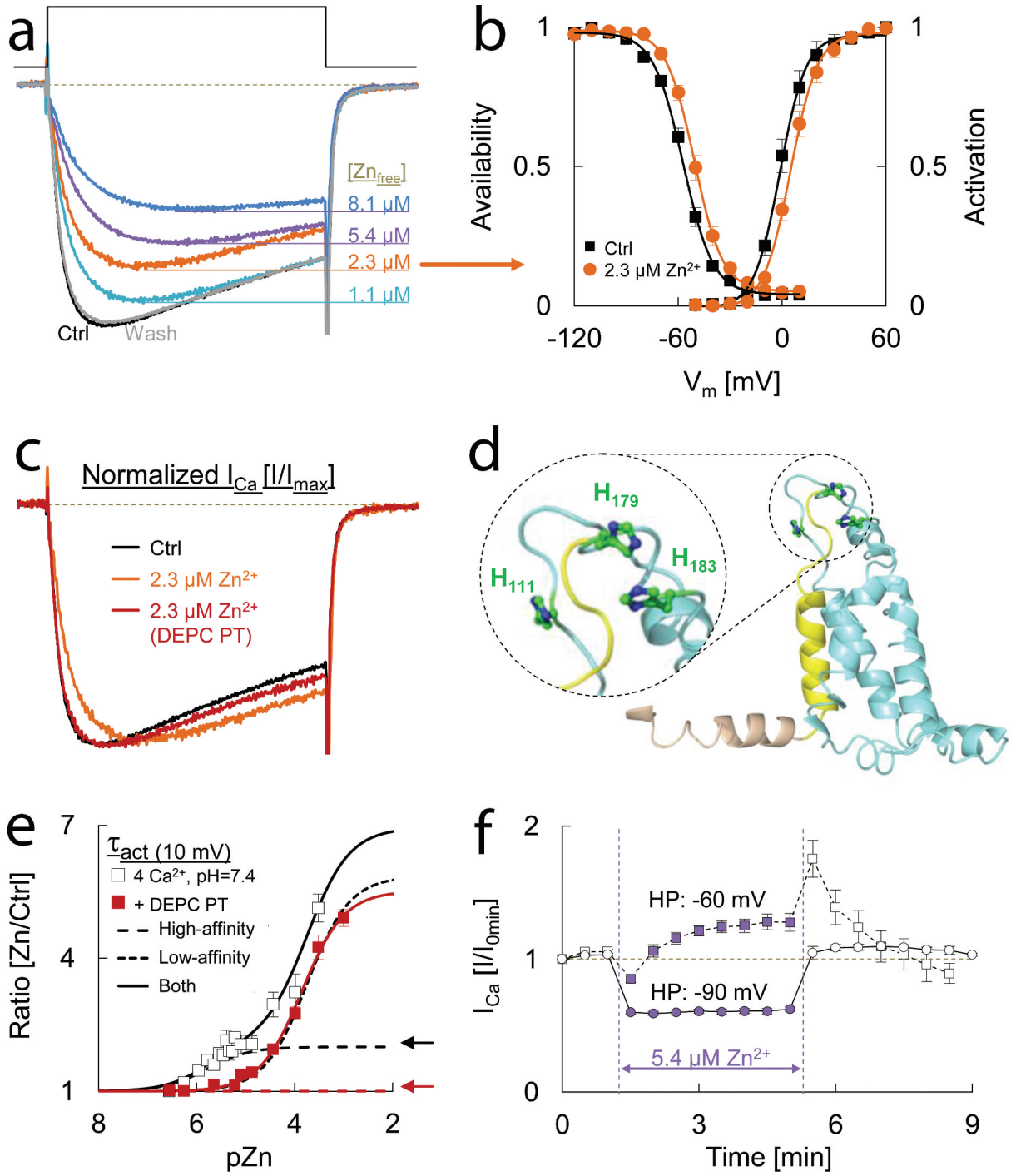

Figure 2. Modulation of $Ca_v2.3$ channel function by low micromolar Zn^{2+} concentrations.

(a) *Concentration-dependent suppression by low micromolar Zn^{2+} of Ca^{2+} currents carried by 4 mM free Ca^{2+} and recorded during a 30 ms voltage-step to 10 mV in HEK293 cells stably transfected with cloned human $Ca_v2.3+\beta_3$ channel complexes.* (b) *Activation (right) and pre-pulse inactivation (left) curves determined in the absence (black squares) and presence (orange circles) of 2.3 µM free Zn^{2+} under the same conditions as in a.* (c) *Macroscopic $Ca_v2.3+\beta_3$ channel currents recorded during a 30 ms voltage-step to 10 mV in the absence (black) or presence (orange) of 2.3 µM free Zn^{2+} and scaled to the same amplitude to illustrate kinetic changes. Also shown are the effects of the same concentration of Zn^{2+} after pre-treatment of cells with the histidine modifying reagent DEPC (red). Note the Zn^{2+}-induced slowing of activation but not deactivation kinetics, which was completely prevented by histidine modification with DEPC.* (d) *Homology model of $Ca_v2.3$ repeat I with the three histidine side chains implicated in high-affinity Zn^{2+}-induced modulation shown as ball and stick representation.* (e) *Concentration-dependence of Zn^{2+}-induced slowing determined under the same conditions as in a (open squares) or after pre-treatment of cells with the histidine modifying reagent DEPC (red squares). Solid lines are the combination of two binding isotherms for simple biomolecular reactions, while dotted lines indicate the corresponding high- and low-affinity components.* (f) *Holding potential (HP)-dependence of Zn^{2+} effects on the amplitude of Ca^{2+} currents evoked by repetitive depolarization to 10 mV.*

$Ca_v2.3$ channels. Thus, at the very negative HPs typically employed to minimize HP-dependent inactivation in electrophysiological recordings, Zn^{2+} rapidly and exclusively suppressed $Ca_v2.3$ channel currents by shifting voltage-dependent activation to more depolarized test potentials and slowing activation (figure 2F). At HPs more positive than −80 mV, where $Ca_v2.3$ channels are subject to processes like ultra-slow closed-state inactivation [50,51], rapid suppression was accompanied by a time-dependent current increase that was also slow to reverse after removal of Zn^{2+}, as reflected in a transient over-recovery of current amplitudes during washout (figure 2f). In the absence of Zn^{2+}, the time-course and degree of current stimulation by a given concentration of free Zn^{2+} could be reproduced by a hyperpolarizing shift in HP equal to the depolarizing shift in channel voltage-dependence produced by that free Zn^{2+} concentration [40], suggesting that it reflects recovery from slow HP-dependent inactivation. That Zn^{2+} reduces slow inactivation would also be in line with the parallel Zn^{2+}-induced changes in activation and fast inactivation (Figures 2(b, c) and could reflect the proposed coupling between activation and inactivation gating [52,53].

Selective permeation and ionic block

When electrophysiological recordings are performed in the absence of Ca^{2+} and other polyvalent cations, VGCCs can mediate large currents carried by monovalent ions like sodium. Addition of micromolar Ca^{2+} potently suppresses these currents in a voltage-dependent manner, which can be well described by assuming that Ca^{2+} blocks the pore through interaction with a high-affinity site located in the membrane electric field [54–58]. Cd^{2+} and lanthanoid block of Ca^{2+} currents have almost the same voltage-dependence and are thought to result from blocker occupation of the same principle intra-pore site [59–65]. In single-channel recordings, these cations produce discrete, long-lasting blocking events [61,66–69], which are consistent with an occlusion of the pore that prevents ion transfer through open channels. Mutational studies have convincingly linked high-affinity Ca^{2+} binding in the pore to a conserved ring of glutamate (and in LVA channels aspartate) residues (EEEE/EEDD-locus) located at equivalent positions in each of the four p-loops [13,70–72]. How high-affinity binding can be reconciled with the high rates of flux observed in the presence of millimolar Ca^{2+} concentrations is less well understood, but thought to involve ion–ion interactions due to simultaneous occupation of the pore by multiple ions [73]. A potential mechanism has been elucidated by construction and crystallographic analysis of the homotetrameric bacterial model channel Ca_vAb and its derivatives [74], in which the selectivity filter is formed by three successive ion-binding sites in the single-file region of the pore (Figure 3a). A central high-affinity Ca^{2+} binding site (site 2) is formed by carboxylate-bearing side chains of aspartate (D_{177}) residues equivalent to the EEEE/EEDD-locus in vertebrate channels and backbone carbonyl groups of neighboring leucine (L_{176}) residues. Consistent with the data on vertebrate channels, site 2 can coordinate a single, hydrated Ca^{2+} (Figure 3a left) or Cd^{2+} (Figure 3b) ion with sufficient affinity for block. It is flanked by two lower-affinity sites formed by carboxylate-bearing side chains of aspartate (D_{178}) residues at the outer edge of the selectivity filter (site 1) and backbone carbonyl groups of threonine (T_{175}) residues on the internal side (site 3) near the central cavity (Figure 3a). High-affinity binding to the central site is thought to be destabilized by repulsive ion–ion interactions when Ca^{2+} ions occupy the two flanking, lower-affinity sites, so that the channel mainly oscillates between two low-energy states in which either one Ca^{2+} ion occupies the central site (Figure 3a left) or two Ca^{2+} ions occupy the two flanking sites (Figure 3a right). Comparison with the modeled human $Ca_v2.3$ channel (Figures 3c-e) shows that sites 2 and 3 are conserved in sequence and 3D space, whereas the architecture of site 1 is distinct from the four-fold symmetric planar ring in Ca_vAb. Thus, in $hCa_v2.3$ (and other HVA channels), only one of the four aspartate residues corresponding to site 1 in Ca_vAb is preserved (D_{615} in repeat II, Figures 3d&e) and has been shown to directly participate in Ca^{2+} interaction with the pore [75]. The remaining three side chains involved in the formation of site 1 in $hCa_v2.3$ appear to be provided by two glutamate (E_{618} in repeat II & E_{1327} in repeat

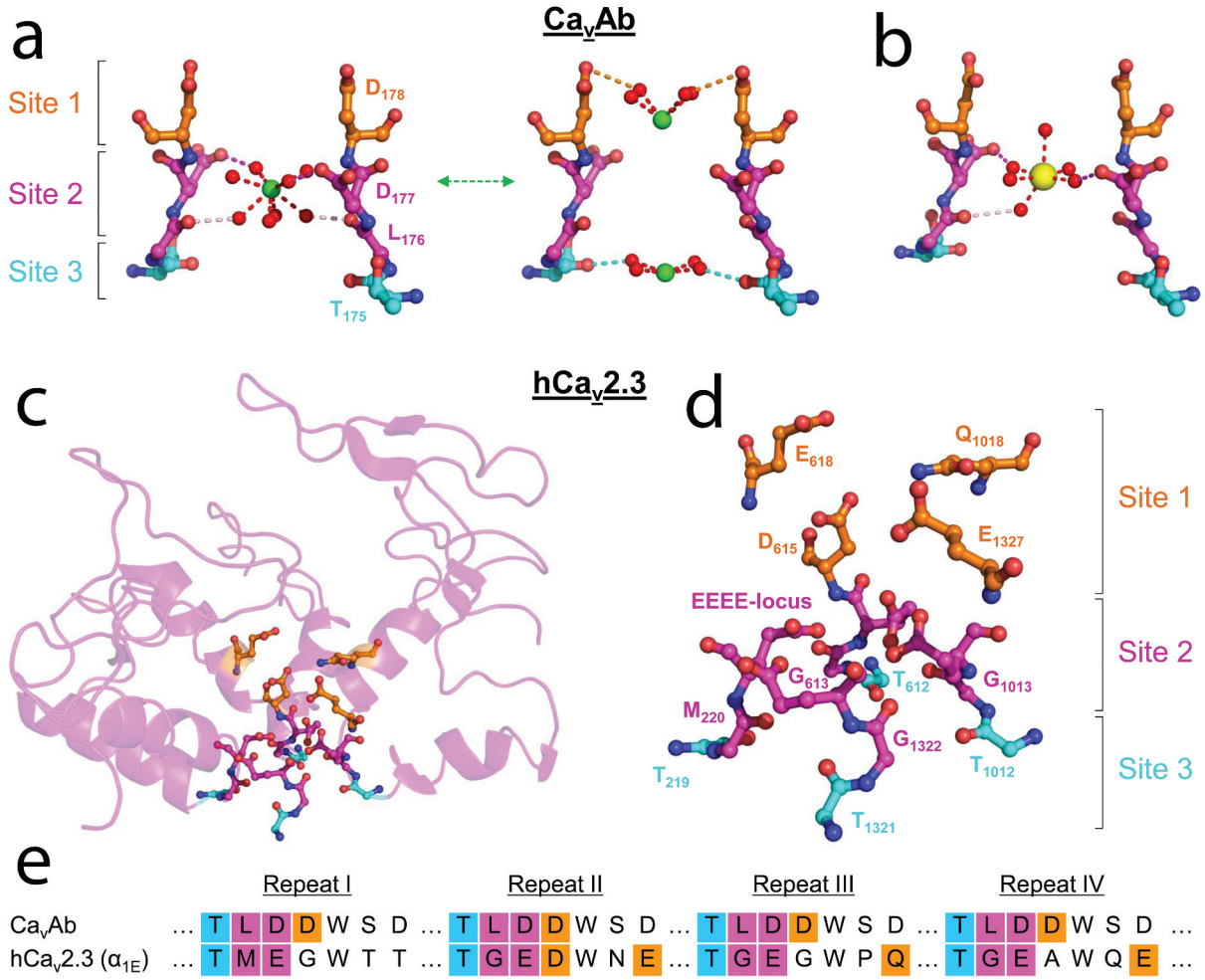

Figure 3. Architecture of the selectivity filter in bacterial Ca_vAb and human $Ca_v2.3$ channels.

(**a-b**) *Ball and stick representation of residues forming the three ion-binding sites in the crystal structure of the bacterial model channel Ca_vAb and its derivatives with* (**a**) *one hydrated Ca^{2+} ion bound to the central high-affinity site (left) or two hydrated Ca^{2+} ions bound to the two flanking low-affinity (right) sites (pdb: 4MS2) or* (**b**) *one hydrated Cd^{2+} ion bound to the central high-affinity site (pdb: 4MVS).* (**c**) *Cartoon representation of the p-loops from three repeats in the homology model of $hCa_v2.3$ with residues corresponding to the three ion-binding sites shown as ball and stick representation.* (**d**) *Close-up view of $hCa_v2.3$ channel residues corresponding to the three ion-binding sites.* (**e**) *Sequence comparison of residues forming the selectivity filter in Ca_vAb and $hCa_v2.3$.*

VI) and one glutamine residue (Q_{1018} in repeat III) from the so-called DCS-locus (Figure 3d), a ring of channel-specific charged residues that participates in selective permeation and ionic block [76,77] and corresponds to residue 181 in Ca_vAb and its derivatives (Figures 3(a, b). Importantly, these structural features could explain a number of previous findings on Ca^{2+} channel block by group IIB metal ions like Zn^{2+} or Cu^{2+}, which has a much shallower voltage-dependence than Cd^{2+} or lanthanoid block and is markedly subunit-dependent, suggesting that it does not take place at the conserved EEEE-locus but at a more superficial, channel-specific site [73]. In addition, these metal ions produce a characteristic slowing of macroscopic activation and deactivation of all native HVA VGCCs, which is closely correlated with their blocking effects but not directly related to the intrinsic properties (i.e. time- and voltage-dependence) of block itself [44,45]. Instead, the slowing has been proposed to involve an allosteric effect on opening and closing that is linked to occupation of the blocking site in the pore. Consistent with this assumption, we have found that both, Zn^{2+}-induced voltage-dependent block (Figure 4a) and the Zn^{2+}-induced low-affinity slowing of cloned $Ca_v2.3$ channels (Figure 4b) described in the preceding section could be

reasonably reproduced by assuming that Zn^{2+}-binding to a single site (K_{Zn}~100 µM) in the pore blocks the channels and slows the opening and closing transitions [40]. Given the many simplifying assumptions of this model, it remains to be determined if both effects are truly mediated by a single site and, if so, whether this site corresponds to site 1 as hypothesized above. Interestingly, our experiments also revealed that Zn^{2+}-induced block is accompanied by a voltage-independent and incomplete suppression of Ca^{2+} influx through open channels with much higher affinity (IC_{50} = 12–16 µM with 4 mM Ca^{2+}) [40]. Histidine-modification with DEPC reduced the degree of high-affinity suppression but increased the degree of block (Figure 4c), suggesting that

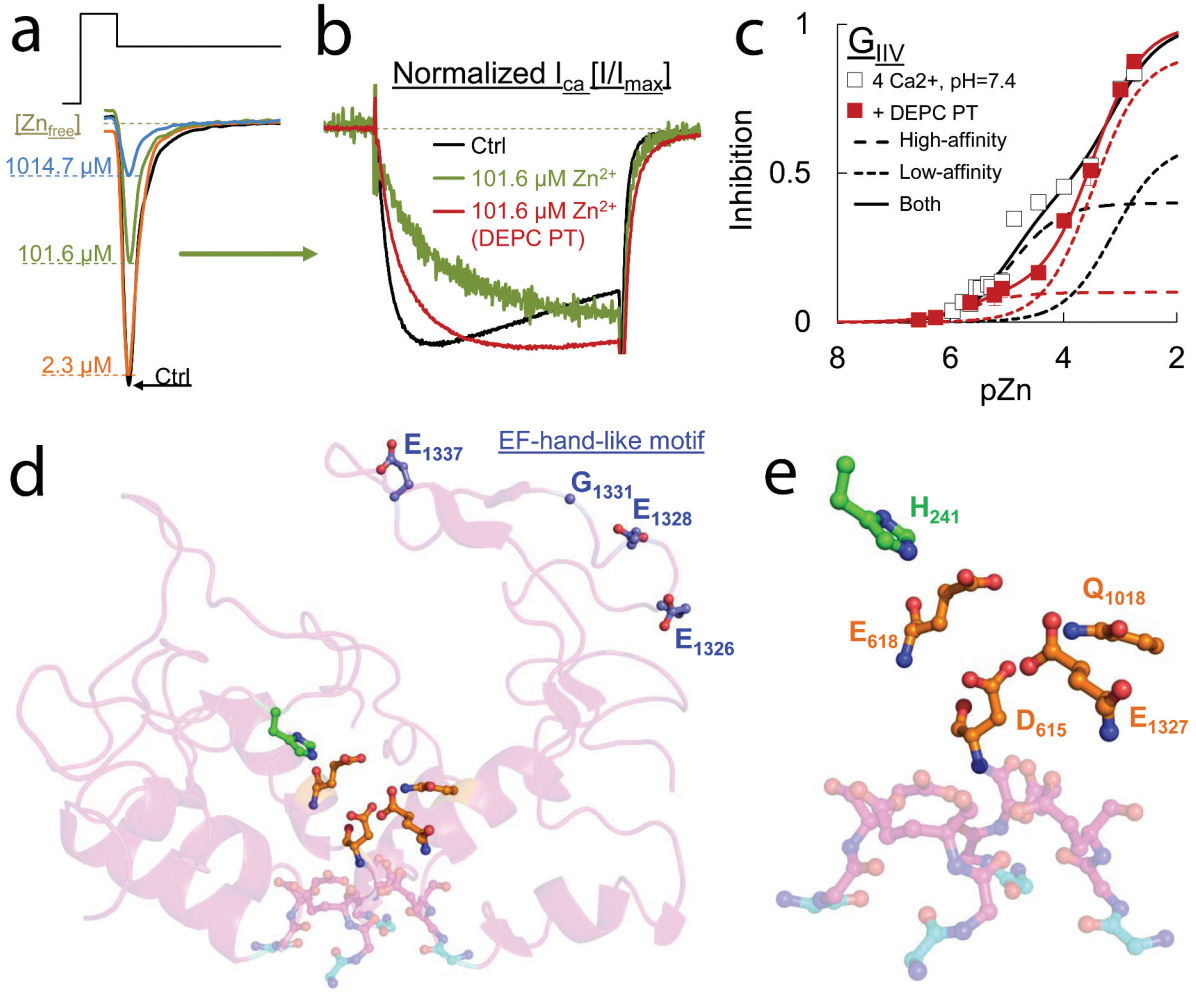

Figure 4. Modulation of $Ca_v2.3$ channel function by high micromolar Zn^{2+} concentrations.

(**a**) *Concentration-dependent suppression by Zn^{2+} of instantaneous currents carried by 4 mM free Ca^{2+} and recorded after channel opening by a depolarizing prepulse in HEK-293 cells stably transfected with cloned human $Ca_v2.3+\beta_3$ channel complexes.* (**b**) *Macroscopic $Ca_v2.3+\beta_3$ channel currents recorded during a 30 ms voltage-step to 10 mV in the absence (black) or presence (green) of 101.6 µM free Zn^{2+} and scaled to the same amplitude to illustrate kinetic changes. Also shown are the effects of the same concentration of free Zn^{2+} after pre-treatment of cells with the histidine modifying reagent DEPC (red). Note the DEPC-resistant Zn^{2+}-induced slowing of both activation and deactivation kinetics.* (**c**) *Concentration-dependence of Zn^{2+}-induced suppression of the instantaneous slope conductance (G_{IIV}) between −40 mV and +20 mV, determined under the same conditions as in A (open squares) or after pre-treatment of cells with the histidine modifying reagent DEPC (red squares). Solid lines are the combination of two binding isotherms for simple biomolecular reactions, while dotted lines indicate the corresponding high- and low-affinity components.* (**d**) *Cartoon representation of the p-loops from three repeats in the homology model of $Ca_v2.3$ with putative residues that could be involved in the blocking and low-affinity gating effects of high micromolar Zn^{2+} shown as ball and stick representation.* (**e**) *Close-up view of residues forming the putative blocking site for group IIB metal ions (orange = site 1 in Fig. 3d) and the nearby histidine residue (green), which has previously been linked to proton-induced changes in unitary conductance.*

occupation of the underlying sites may be mutually exclusive. In this context, it is interesting that protons have been shown to reduce $Ca_v2.3$ channel unitary conductance by interaction with a non-conserved histidine residue (His_{241}) in the p-loop of repeat I [47], which is located directly adjacent to site 1 (Figures 4(d, e). This makes it tempting to speculate that interaction of Zn^{2+} with the same residue might reduce the net charge density and/or cross-sectional area available for passage of other ions without complete occlusion of the pore, which could explain the DEPC-sensitivity and incomplete nature of the high-affinity component. Moreover, considering its close spatial proximity to site 1, Zn^{2+} occupation of His_{241} would be expected to reduce the probability that another Zn^{2+} ion occupies site 1. That said, the multiple effects of Zn^{2+} on $Ca_v2.3$ channel gating and permeation are evidently complex, and further studies will be required for a clear separation and throughout understanding of the underlying mechanisms. Thus, a putative EF-hand motif in the p-loop of domain III of all HVA channels (Figure 4d) has previously been implicated in their differential sensitivity to Zn^{2+}-block as well [78,79] and its absence in LVA channels could explain why a prominent Zn^{2+}-induced slowing is only observed in HVA channels. On the other hand, the superficial location of this site (Figure 4d) is difficult to reconcile with an occlusion of the pore, so that it may not be directly involved in Zn^{2+}-induced block. Another relevant question that will be discussed in section 4 is if voltage-dependent block and low-affinity slowing could ever become relevant under (patho)physiological conditions, or if they are simply phenomena that have to be taken into account when studying the effects of trace metals on $Ca_v2.3$ channel function.

$Ca_v2.3$ channel expression and relevance in different tissues

$Ca_v2.3$ channels are widely expressed throughout the central and peripheral nervous system [37,64,80,81] and in endocrine [80,82,83], cardiovascular [84], gastrointestinal [80] and reproductive tissues [85,86]. Despite this widespread expression, $Ca_v2.3$-deficient mice display a surprisingly subtle phenotype with no major pathologies but altered nociception [87], glucose homeostasis [49,88,89] and spatial memory [90], impaired autonomic control [84,91], increased anxiety [92] and reduced susceptibility to chemically induced seizures [93,94].

$Ca_v2.3$ channels in the central nervous system

In the brain, highest densities of $Ca_v2.3$ channels have been detected in the hippocampus and other limbic regions, in the neocortex and in the retina [95,96]. They are expressed in pre- and post-synaptic neurons [97,98] and have been shown to play a role for neurotransmitter release, synaptic plasticity, action potential burst firing and somatodendritic integration [99–106]. In the retina, Ca^{2+}-influx through $Ca_v2.3$ channels has been linked to GABAergic reciprocal inhibition of rod ON-bipolar cells as part of the scotopic visual pathway [107]. The exact physiological relevance of $Ca_v2.3$ channels in most other brain regions remains elusive, but they have been implicated in a number of pathophysiological conditions. Most notably, $Ca_v2.3$ channels are thought to play a pro-ictogenic role in convulsive-generalized tonic-clonic and hippocampal seizures, since their genetic ablation reduces the susceptibility to chemically induced seizures [93,94,108] and abrogates the effects of several broad-spectrum antiepileptic drugs known to suppress cloned $Ca_v2.3$ channels [94,109,110]. More recently, de novo gain-of-function mutations in $Ca_v2.3$ channels have also been linked to developmental and epileptic encephalopathies in human patients, which are associated with epileptiform EEG activity, intractable seizures, and developmental impairments [111,112].

$Ca_v2.3$ channels in the endocrine pancreas

A number of studies have linked $Ca_v2.3$ channels to α-cell glucagon [49,113], β-cell insulin [88,89,114], and δ-cell somatostatin (SST) secretion [115] in pancreatic islets, suggesting that they are involved in the regulation of blood glucose homeostasis. During hyperglycemia, glucose homeostasis is mainly maintained by glucose-stimulated insulin secretion (GSIS), which can be separated into a first phase mediated by fast secretion of insulin from a readily releasable pool of vesicles and a second phase of sustained release

that is thought to involve mobilization of a reserve pool of vesicles [114]. Genetic or pharmacological ablation of $Ca_v2.3$ channels in mice has been shown to selectively reduce the second-phase insulin response [113,114], suggesting that they are involved in the mobilization of insulin vesicles from the reserve pool. In addition, SST has been shown to inhibit cloned $Ca_v2.3$ channels [116] and SNX-482 prevents SST inhibition of insulin secretion from insulinoma cells [117], indicating that β-cell $Ca_v2.3$ channels could also play a role for the regulation of insulin secretion by SST. According to the intra-islet insulin hypothesis, insulin released from β-cells during hyperglycemia could tonically suppress glucagon release from downstream α-cells, so that cessation of insulin release during hypoglycemia serves as a switch-off signal that initiates α-cell glucagon secretion [118,119]. Interestingly, glucose-induced suppression of glucagon release is severely impaired in $Ca_v2.3$-deficient mice [114], in isolated islets from $Ca_v2.3$-deficient mice [113,114] and in SNX-482 treated islets from wild-type mice [114,120], but SNX-482 fails to suppress glucagon secretion from wild-type islets in low glucose and fasting glucagon levels are significantly higher in $Ca_v2.3$-deficient compared to wild-type mice [49]. Taken together, these findings suggest that $Ca_v2.3$ channels are important for suppression of glucagon release during hyperglycemia but not strictly required for the release of glucagon during hypoglycemia.

$Ca_v2.3$ channels in reproductive tissues

During passage of sperm through the female reproductive tract, spermatozoa undergo a series of chemical and physiological changes collectively called capacitation, which are required for acrosome exocytosis (AE) and the subsequent steps of oocyte fertilization. Capacitation is associated with changes in membrane lipid composition, increased intracellular Ca^{2+} levels, membrane hyperpolarization, activation of second messenger systems and a unique sperm motility pattern [85,121–124]. The underlying mechanisms are still incompletely understood, but Ca^{2+} influx through $Ca_v2.3$ channels secondary to focal enrichment of the ganglioside G_{M1} has been shown to promote capacitation [85] and sperm from $Ca_v2.3$-deficient mice exhibits altered Ca^{2+} responses, aberrant motility, reduced acrosome exocytosis, and a strong subfertility phenotype [85,125].

4. (Patho)physiological implications of Zn^{2+} induced $Ca_v2.3$ channel modulation

Although the role of vesicular Zn^{2+} has been most extensively studied in the central nervous system, loosely bound Zn^{2+} is also important in the peripheral nervous system and in neuroendocrine and reproductive tissues. Due to a large concentration-gradient favoring passive entry, released Zn^{2+} can usually gain access to the intracellular compartment as well, which is under study as a potential neuronal signaling pathway [126] and has been implicated in cell death under certain pathophysiological conditions [4,127,128]. Since $Ca_v2.3$ channels are unlikely to play a role for cellular Zn^{2+} entry [73,129], the rest of the present article will focus on the role and effects of extracellular loosely bound Zn^{2+} in different tissues.

$Ca_v2.3$ channels as a target for synaptic Zn^{2+} signals in the brain

Loosely bound Zn^{2+} accounts for roughly 10% of total brain Zn^{2+}, and is almost exclusively located in the presynaptic vesicles of so-called zinc-enriched neurons [3,4]. These neurons are not associated with a single neurotransmitter and mainly located in the limbic system, the neocortex and the retina [130–132], which coincides almost exactly with the expression pattern of $Ca_v2.3$ channels in the brain. Resting levels of loosely bound Zn^{2+} in the brain extracellular fluid are in the order of 5–25 nM [133], but these values are frequently exceeded at the synapses of zinc-enriched neurons, although the exact magnitude of synaptic Zn^{2+} signals remains a matter of debate. Based on experiments in acute brain slices, some have estimated that peak cleft concentrations at hippocampal mossy fiber synapses could be in the order of 10–20 μM during basal synaptic activity and in excess of 100 μM during more intense, LTP-inducing stimulation [134], while others have questioned that they could even exceed 1 μM [135,136]. However, based on a large number of studies [126,137–146] and taking into account that Zn^{2+} release is

substantially reduced in acute brain slices [147], it seems reasonable to assume that physiological Zn^{2+} signals in the brain are in the low micromolar concentration range, so that $Ca_v2.3$ channel modulation occurs mainly via high-affinity binding. The exact functional relevance of synaptic Zn^{2+} remains controversial as well, but it has been implicated in several physiological and pathophysiological processes. For example, using the rapid Zn^{2+} chelator ZX1 and different strains of knockout mice, synaptic Zn^{2+} has been shown exert a dual control of non-NMDA receptor-dependent long-term potentiation (LTP) in hippocampal mossy fiber-CA3 synapses, where it promotes induction of presynaptic and inhibits induction of postsynaptic LTP [148]. Presynaptic LTP induction at these synapses involves Ca^{2+} influx through $Ca_v2.3$ channels [100,149], suggesting that they could play a role for the effects of Zn^{2+}. Interestingly however, Zn^{2+} chelation by ZX1 [148] produced the same effects as genetic or pharmacological ablation of $Ca_v2.3$ channels [100,149], namely a decrease of LTP induction without changes in LTP expression, basal transmission, paired-pulse facilitation or frequency facilitation. These results are difficult to explain by a ZX1-induced reversal of Zn^{2+}-induced suppression but could be reconciled by our recent finding that low micromolar Zn^{2+} can also stimulate $Ca_v2.3$ channel function [40]. Thus, assuming that the (local) resting membrane potential (RMP) is sufficiently positive (>-70 mV) that a significant fraction of the channels is inactivated, synaptic Zn^{2+} could increase Ca^{2+} influx by increasing the fraction of channels available for activation, in which case Zn^{2+} chelation should mimic the effects of $Ca_v2.3$ channel ablation. The dual effects of Zn^{2+} on mossy fiber LTP have been proposed to support physiological functions while preventing hyperexcitability due to excessive activation of CA3 pyramids [44,45]. A number of experimental and clinical findings support the view that synaptic Zn^{2+} could serve as an intrinsic anticonvulsant that dampens excitability not only in limbic brain regions. For example, synaptic release and extracellular accumulation of Zn^{2+} in mice have been demonstrated to limit the propagation of cortical spreading depression *in vitro* and *in vivo* [150] and Zn^{2+} treatment reduced dentate granule cell hyperexcitability in human epileptic patients [151]. Zn^{2+} deficiency or chelation have conversely been shown to increase the susceptibility to chemically induced seizures in mice or rats [152,153] and to induce seizures and excitotoxicity in healthy rats [154] and rats subjected to non-lesioning over-excitation [155]. Given their apparently pro-ictogenic role, $Ca_v2.3$ channels would represent an optimal target for the anticonvulsant action of vesicular Zn^{2+} under pathophysiological conditions. Zn^{2+} levels in the extracellular space during chemically induced epileptiform discharges have been estimated to be in the order of 300 μM [139], so that pore block and low-affinity slowing could significantly contribute to Zn^{2+}-induced $Ca_v2.3$ channel modulation under pathophysiological conditions. The latter could be important to prevent excessive Ca^{2+} influx when over-excitation leads to a depolarization of the neuronal RMP, as it would counteract the reversal of RMP-dependent inactivation mediated by high-affinity Zn^{2+} binding. However, given its many molecular targets, the net effect of Zn^{2+} treatment or chelation on brain function can clearly not be attributed to changes in $Ca_v2.3$ channel gating and permeation alone. For example, Zn^{2+} has also been shown to slow the deactivation kinetics of LVA $Ca_v3.3$ channels [156] and even submicromolar concentrations potently inhibit $Ca_v3.2$ channels [42,156,157] as well as certain neurotransmitter receptors [158,159] and possibly other targets.

$Ca_v2.3$ channels as a target for paracrine Zn^{2+} signals in the pancreas

β-cell insulin secretory granules contain high (millimolar) concentrations of Zn^{2+}, which forms 2Zn-hexameric complexes with insulin and is well known to be required for proper insulin biosynthesis, maturation, and secretion [160,161]. After release into the periportal circulation, the higher pH of blood leads to rapid dissociation into free Zn^{2+} and insulin monomers [161,162], which has been estimated to transiently raise the local Zn^{2+} concentration to several hundreds of micromolar [128]. Based on these and other findings, Zn^{2+} has been proposed as a candidate signal for non-insulin paracrine intra-islet crosstalk to nearby α-cells [5]. Thus, according to the Zn^{2+} switch-off hypothesis, β-cell Zn^{2+} release during hyperglycemia could tonically suppress glucagon secretion by opening α-cell K_{ATP} and inhibiting α-

cell Ca^{2+} and Na^{+} channels, whereas cessation of Zn^{2+} supply during hypoglycemia could lead to closure of K_{ATP} channels and Na^{+} and L-type Ca^{2+} channel-dependent firing of action potentials (APs), during the peaks of which local Ca^{2+}-influx through P/Q-type Ca^{2+} channels triggers glucagon secretion. Support for this hypothesis is provided by findings that Zn^{2+} suppresses pyruvate- or glucose-induced glucagon release in static secretion and electrophysiological experiments with isolated rodent islets and purified α-cells [163,164]. In addition, Zn^{2+} but not Zn^{2+}-free insulin was reported to inhibit α-cell glucagon secretion in the perfused rat pancreas [162,165], although some studies failed to detect Zn^{2+}-induced suppression of glucagon secretion [166,167]. Consistent with a role of Zn^{2+} and $Ca_v2.3$ channels for the regulation of glucagon release, we have previously shown that *in vivo* Zn^{2+} chelation produces a correlated increase of blood glucose and serum glucagon levels in wild-type mice, and that this response is severely blunted in $Ca_v2.3$-deficient mice [49]. In addition, fasting glucose and glucagon levels were significantly higher in $Ca_v2.3$-deficient compared to wild-type mice [49], suggesting that deficiency of these channels impairs the coupling between blood glucose levels and glucagon secretion without reducing glucagon release per se. One explanation for these findings could be that Zn^{2+} dis-inhibition of $Ca_v2.3$ channels serves to amplify the effects of K_{ATP} channel closure and alters P/Q-type channel-dependent exocytosis by modifying the threshold or peak height of α-cell APs, without being a critical requirement for α-cell glucagon secretion per se. Alternatively, considering the relatively depolarized α-cell RMP, Zn^{2+} release during hyperglycemia could simultaneously suppress $Ca_v2.3$ channels and increase their availability for activation at rest, so that rapid reversal of Zn^{2+}-induced suppression upon cessation of Zn^{2+} supply allows for a brief burst of Ca^{2+} influx prior to time-dependent reentry into inactivated states. The latter could be an attractive mechanism by which (cessation of) Zn^{2+} release from β-cells synchronizes the pulsatile release of insulin and glucagon. Finally, it has also been proposed that the suppression of glucagon secretion during hyperglycemia results from depolarization-induced inactivation of Na^{+} and Ca^{2+} channels due to α-cell glucose metabolism and closure of K_{ATP} channels, which reduces the AP peak height and thus P/Q-type Ca^{2+} channel-mediated exocytosis, while electrical activity and global Ca^{2+} oscillations remain preserved [120,168,169]. In this view, the Zn^{2+}-induced depolarizing shift in $Ca_v2.3$ channel voltage-dependence might allow them to remain active during hyperglycemia, so that they could be involved in maintaining α-cell electrical activity and global Ca^{2+} oscillations. In any case, we interestingly also found that glucose tolerance is preserved in vehicle-treated but severely impaired in Zn^{2+}-chelated $Ca_v2.3$-deficient mice [49], suggesting that adequate Zn^{2+} levels are critical for maintaining glucose tolerance under conditions of $Ca_v2.3$ channel dysfunction. The latter finding could have important clinical implications, as the region of the human $Ca_v2.3$ gene has been linked to impaired glucose homeostasis in human patients with type 2 diabetes mellitus [170–172], which could possibly benefit from Zn^{2+} supplementation.

$Ca_v2.3$ channels as a target for Zn^{2+} signals in reproductive tissues

When compared to blood plasma (~11-23 μM total and 0.1–1 nM loosely bound Zn^{2+}) [173,174], human seminal plasma contains exceptionally high concentrations of Zn^{2+} (~2-3 mM total Zn^{2+}) [175,176], which is mainly secreted by the prostate [177] and plays a vital role in sperm capacitation [176]. The high Zn^{2+} concentrations in seminal plasma are thought to be an important gatekeeper for maintaining sperm in a metabolically quiescent state, whereas the decrease in Zn^{2+} concentration due to filtering out of seminal fluid in the female reproductive tract could promote capacitation [176]. In addition, sperm-induced Zn^{2+} release from the oocyte, the so-called Zn^{2+} sparks, could be involved in preventing the entry of more than one spermatozoon at fertilization [176,178,179]. Unfortunately, the exact concentration of loosely bound Zn^{2+} in seminal plasma has not been determined, but estimated to be in the order of at least 3 μM [175], suggesting that high-affinity modulation of $Ca_v2.3$ channels could contribute to the effects of Zn^{2+}. In this context, it is especially interesting that acrosome exocytosis has been shown to depend on spatiotemporal information encoded by a transient burst of Ca^{2+} influx through $Ca_v2.3$ channels and not the mere presence or amplitude of Ca^{2+} waves [85]. Based on the depolarized RMP of non-capacitated

sperm, Zn^{2+} could not only suppress $Ca_v2.3$ channels but also increase their availability for activation. During the passage of the female reproductive tract and filtering out of seminal fluid, rapid reversal of Zn^{2+}-induced suppression could allow for a transient influx of Ca^{2+} through these channels, which is subsequently terminated by time-dependent inactivation, as exemplified by the time-course of changes upon Zn^{2+} removal in (figure 2F). Presumably, however, a complex interplay exists between gradual changes in Zn^{2+} concentration, RMP, and membrane lipid composition during passage of the female reproductive tract, which could fine-tune the temporal profile of Ca^{2+} influx through $Ca_v2.3$ channels during different stages of the reproductive process.

Conclusion

Although the exact functional role of Zn^{2+}-induced $Ca_v2.3$ channel modulation in most tissues remains to be firmly established, the picture that emerges is one where $Ca_v2.3$ channel expression parallels the occurrence of loosely bound Zn^{2+} pools, and where these channels may serve to translate physiological Zn^{2+} signals into changes of electrical activity and/or intracellular Ca^{2+} levels. Improved tools for investigation of endogenous Zn^{2+} signals and genetic approaches to identify and manipulate the different putative Zn^{2+} binding sites will be required to understand their function and contribution to Zn^{2+}-induced $Ca_v2.3$ channel modulation in different tissues.

Disclosure statement

No potential conflict of interest was reported by the authors.

ORCID

Felix Neumaier http://orcid.org/0000-0002-6376-6391
Toni Schneider http://orcid.org/0000-0003-2816-2696
Walid Albanna http://orcid.org/0000-0001-9986-8739

References

[1] Anzellotti AI, Farrell NP. Zinc metalloproteins as medicinal targets. Chem Soc Rev. 2008;37(8):1629.
[2] Frederickson CJ, Koh J-Y, Bush AI. The neurobiology of zinc in health and disease. Nat Rev Neurosci. 2005;6:449–462.
[3] Frederickson CJ, Suh SW, Silva D, et al. Importance of zinc in the central nervous system: the zinc-containing neuron. J Nutr. 2000;130(5):1471S–83S.
[4] Mathie A, Sutton GL, Clarke CE, et al. Zinc and copper: pharmacological probes and endogenous modulators of neuronal excitability. Pharmacol Ther. 2006;111(3):567–583.
[5] Ishihara H, Maechler P, Gjinovci A, et al. Islet beta-cell secretion determines glucagon release from neighbouring alpha-cells. Nat Cell Biol. 2003;5(4):330–335.
[6] Suh SW, Chen JW, Motamedi M, et al. Evidence that synaptically-released zinc contributes to neuronal injury after traumatic brain injury. Brain Res. 2000;852(2):268–273.
[7] Pringos E, Vignes M, Martinez J, et al. Peptide neurotoxins that affect voltage-gated calcium channels: a close-up on omega-agatoxins. Toxins (Basel). 2011;3(1):17–42.
[8] Tottene A, Volsen S, Pietrobon D. α_{1E} subunits form the pore of three cerebellar R-type calcium channels with different pharmacological and permeation properties. J Neurosci. 2000;20(1):171–178.
[9] Bourinet E, Stotz SC, Spaetgens RL, et al. Interaction of SNX482 with domains III and IV inhibits activation gating of α_{1E} ($Ca_v2.3$) calcium channels. Biophys J. 2001;81(1):79–88.
[10] Martinez-Ortiz W, Cardozo TJ. An improved method for modeling voltage-gated ion channels at atomic accuracy applied to human Ca_v channels. Cell Rep. 2018;23(5):1399–1408.
[11] Zhen X, Xie C, Fitzmaurice A, et al. Functional architecture of the inner pore of a voltage-gated Ca^{2+} channel. J Gen Physiol. 2005;126(3):193–204.
[12] Kim M-S, Morii T, Sun L-X, et al. Structural determinants of ion selectivity in brain calcium channel. FEBS Lett. 1993;318(2):145–148.
[13] Yang J, Ellinor PT, Sather WA, et al. Molecular determinants of Ca^{2+} selectivity and ion permeation in L-type Ca^{2+} channels. Nature. 1993;366(6451):158-161.
[14] Snutch TP, Peloquin J, Mathews E, et al. Molecular properties of voltage-gated calcium channels. In: Voltage-gated calcium channels. Boston, MA: Springer US; 2005. p. 61–94.
[15] Bezanilla F. The voltage sensor in voltage-dependent ion channels. Physiol Rev. 2000;80(2):555–592.
[16] Bezanilla F. Voltage sensor movements. J Gen Physiol. 2002;120:465–473.
[17] Josephson IR, Varadi G. The beta subunit increases Ca^{2+} currents and gating charge movements of human cardiac L-type Ca^{2+} channels. Biophys J. 1996;70(3):1285–1293.
[18] Jones LP, Wei S-K, Yue DT. Mechanism of auxiliary subunit modulation of neuronal α_{1E} calcium channels. J Gen Physiol. 1998;112(2):125–143.

[19] Neely A, Wei X, Olcese R, et al. Potentiation by the beta subunit of the ratio of the ionic current to the charge movement in the cardiac calcium channel. Science. 1993;262(5133):575–578.
[20] Kamp TJ, Pérez-García MT, Marban E. Enhancement of ionic current and charge movement by coexpression of calcium channel beta 1A subunit with alpha 1C subunit in a human embryonic kidney cell line. J Physiol. 1996;492(1):89–96.
[21] Chanda B, Bezanilla F. Tracking voltage-dependent conformational changes in skeletal muscle sodium channel during activation. J Gen Physiol. 2002;120 (5):629–645.
[22] Chen LQ, Santarelli V, Horn R, et al. A unique role for the S4 segment of domain 4 in the inactivation of sodium channels. J Gen Physiol. 1996;108(6):549–556.
[23] Capes DL, Goldschen-Ohm MP, Arcisio-Miranda M, et al. Domain IV voltage-sensor movement is both sufficient and rate limiting for fast inactivation in sodium channels. J Gen Physiol. 2013;142(2):101–112.
[24] Goldschen-Ohm MP, Capes DL, Oelstrom KM, et al. Multiple pore conformations driven by asynchronous movements of voltage sensors in a eukaryotic sodium channel. Nat Commun. 2013;4(1):1350.
[25] Hodgkin AL, Huxley AF. A quantitative description of membrane current and its application to conduction and excitation in nerve. J Physiol. 1952;117(4):500–544.
[26] Hodgkin AL, Huxley AF. The components of membrane conductance in the giant axon of Loligo. J Physiol. 1952;116(4):473–496.
[27] Sala F. Activation kinetics of calcium currents in bullfrog sympathetic neurones. J Physiol. 1991;437 (1):221–238.
[28] Kostyuk PG, Krishtal OA, Shakhovalov YA. Separation of sodium and calcium currents in the somatic membrane of mollusc neurones. J Physiol. 1977;270(3):545–568.
[29] Kay AR, Wong RK. Calcium current activation kinetics in isolated pyramidal neurones of the CA1 region of the mature guinea-pig hippocampus. J Physiol. 1987;392(1):603–616.
[30] Benison G, Keizer J, Chalupa LM, et al. Modeling temporal behavior of postnatal cat retinal ganglion cells. J Theor Biol. 2001;210(2):187–199.
[31] Pantazis A, Savalli N, Sigg D, et al. Functional heterogeneity of the four voltage sensors of a human L-type calcium channel. Proc Natl Acad Sci. 2014;111 (51):18381–18386.
[32] Savalli N, Pantazis A, Sigg D, et al. The $\alpha_2\delta_1$ subunit remodels $Ca_v1.2$ voltage sensors and allows Ca^{2+} influx at physiological membrane potentials. J Gen Physiol. 2016;148(2):147–159.
[33] Flucher BE. Specific contributions of the four voltage-sensing domains in L-type calcium channels to gating and modulation. J Gen Physiol. 2016;148(2):91–95.
[34] Beyl S, Hohaus A, Andranovits S, et al. Upward movement of IS4 and IIIS4 is a rate-limiting stage in $Ca_v1.2$ activation. Pflügers Arch - Eur J Physiol. 2016;468(11–12):1895–1907.
[35] García J, Nakai J, Imoto K, et al. Role of S4 segments and the leucine heptad motif in the activation of an L-type calcium channel. Biophys J. 1997;72(6):2515–2523.
[36] Fass DM, Levitan ES. L-type Ca^{2+} channels access multiple open states to produce two components of Bay K 8644-dependent current in GH3 cells.. J Gen Physiol. 1996;108(1):13–26.
[37] Schneider T, Wei X, Olcese R, et al. Molecular analysis and functional expression of the human type E neuronal Ca^{2+} channel alpha 1 subunit. Recept Channels. 1994;2:255–270.
[38] Nakayama S, Brading AF. Evidence for multiple open states of the Ca^{2+} channels in smooth muscle cells isolated from the guinea-pig detrusor.. J Physiol. 1993;471(1):87–105.
[39] Josephson IR. Kinetic components of the gating currents of human cardiac L-type Ca $^{2+}$ channels. Pflügers Arch Eur J Physiol. 1997;433(3):321–329.
[40] Neumaier F, Alpdogan S, Hescheler J, et al. Zn^{2+}-induced changes in $Ca_v2.3$ channel function: an electrophysiological and modeling study. J Gen Physiol. 2020;152(9):e202012585.
[41] Zamponi GW, Bourinet E, Snutch TP. Nickel block of a family of neuronal calcium channels: subtype- and subunit-dependent action at multiple sites. J Membr Biol. 1996;151(1):77–90.
[42] Shcheglovitov A, Vitko I, Lazarenko RM, et al. Molecular and biophysical basis of glutamate and trace metal modulation of voltage-gated $Ca_v2.3$ calcium channels. J Gen Physiol. 2012;139:219–234.
[43] Kang H-W, Moon HJ, Joo SH, et al. Histidine residues in the IS3-IS4 loop are critical for nickel-sensitive inhibition of the Ca_v 2.3 calcium channel. FEBS Lett. 2007;581(30):5774–5780.
[44] Castelli L, Tanzi F, Taglietti V, et al. Cu^{2+}, Co^{2+}, and Mn^{2+} modify the gating kinetics of high-voltage-activated Ca^{2+} channels in rat palaeocortical neurons. J Membr Biol. 2003;195(3):121–136.
[45] Magistretti J, Castelli L, Taglietti V, et al. Dual effect of Zn^{2+} on multiple types of voltage-dependent Ca^{2+} currents in rat palaeocortical neurons. Neuroscience. 2003;117(2):249–264.
[46] Magistretti J, Brevi S, De Curtis M. Ni^{2+} slows the activation kinetics of high-voltage-activated Ca^{2+} currents in cortical neurons: evidence for a mechanism of action independent of channel-pore block. J Membr Biol. 2001;179(3):243–262.
[47] Cens T, Rousset M, Charnet P. Two sets of amino acids of the domain I of $Ca_v2.3$ Ca^{2+} channels contribute to their high sensitivity to extracellular protons. Pflügers Arch Eur J Physiol. 2011;462(2):303–314.

[48] Neumaier F, Akhtar-Schäfer I, Lüke JN, et al. Reciprocal modulation of Ca_v 2.3 voltage-gated calcium channels by copper(II) ions and kainic acid. J Neurochem. 2018;147(3):310–322.
[49] Drobinskaya I, Neumaier F, Pereverzev A, et al. Diethyldithiocarbamate-mediated zinc ion chelation reveals role of Ca_v2.3 channels in glucagon secretion. Biochim Biophys Acta Mol Cell Res. 2015;1853 (5):953–964.
[50] Boyett MR, Honjo H, Harrison SM, et al. Ultra-slow voltage-dependent inactivation of the calcium current in guinea-pig and ferret ventricular myocytes. Pflügers Arch Eur J Physiol. 1994;428(1):39–50.
[51] Yasuda T, Lewis RJ, Adams DJ. Overexpressed $Ca_v\beta_3$ inhibits N-type (Ca_v2.2) calcium channel currents through a hyperpolarizing shift of "ultra-slow" and "closed-state" inactivation. J Gen Physiol. 2004;123 (4):401–416.
[52] Serrano JR, Perez-Reyes E, Jones SW. State-dependent inactivation of the alpha1G T-type calcium channel. J Gen Physiol. 1999;114(2):185–201.
[53] Talavera K, Nilius B. Evidence for common structural determinants of activation and inactivation in T-type Ca^{2+} channels. Pflügers Arch Eur J Physiol. 2006;453:189–201.
[54] Fukushima Y, Hagiwara S. Currents carried by monovalent cations through calcium channels in mouse neoplastic B lymphocytes. J Physiol. 1985;358 (1):255–284.
[55] Lux H-D, Carbone E, Zucker H. Na^+ currents through low-voltage-activated Ca^{2+} channels of chick sensory neurones: block by external Ca^{2+} and Mg^{2+}. J Physiol. 1990;430(1):159–188.
[56] Carbone E, Lux H-D, Carabelli V, et al. Ca2+ and Na + permeability of high-threshold Ca2+ channels and their volt age-dependent block by Mg2+ ions in chick sensory neurones. J Physiol. 1997;504(1):1–15.
[57] Shcheglovitov A, Kostyuk P, Shuba YM. Selectivity signatures of three isoforms of recombinant T-type Ca^{2+} channels. Biochim Biophys Acta - Biomembr. 2007;1768(6):1406–1419.
[58] Khan N, Gray IP, Obejero-Paz CA, et al. Permeation and gating in Ca_v3.1 (alpha1G) T-type calcium channels effects of Ca^{2+}, Ba^{2+}, Mg^{2+}, and Na^+. J Gen Physiol. 2008;132:223–238.
[59] Lansman JB, Hess P, Tsien RW. Blockade of current through single calcium channels by Cd^{2+}, Mg^{2+}, and Ca^{2+}. Voltage and concentration dependence of calcium entry into the pore. J Gen Physiol. 1986;88 (3):321–347.
[60] Huang Y, Quayle JM, Worley JF, et al. External cadmium and internal calcium block of single calcium channels in smooth muscle cells from rabbit mesenteric artery. Biophys J. 1989;56(5):1023–1028.
[61] Lansman JB. Blockade of current through single calcium channels by trivalent lanthanide cations. Effect of ionic radius on the rates of ion entry and exit. J Gen Physiol. 1990;95(4):679–696.
[62] Lacinová L, Klugbauer N, Hofmann F. Regulation of the calcium channel alpha(1G) subunit by divalent cations and organic blockers. Neuropharmacology. 2000;39(7):1254–1266.
[63] Díaz D, Bartolo R, Delgadillo DM, et al. Contrasting effects of Cd^{2+} and Co^{2+} on the blocking/unblocking of human Ca_v3 channels. J Membr Biol. 2005;207 (2):91–105.
[64] Williams ME, Marubio LM, Deal CR, et al. Structure and functional characterization of neuronal alpha 1E calcium channel subtypes. J Biol Chem. 1994;269:22347–22357.
[65] Rosenberg RL, Hess P, Tsien RW. Cardiac calcium channels in planar lipid bilayers. L-type channels and calcium-permeable channels open at negative membrane potentials. J Gen Physiol. 1988;92(1):27–54.
[66] Mlinar B, Enyeart JJ. Block of current through T-type calcium channels by trivalent metal cations and nickel in neural rat and human cells. J Physiol. 1993;469(1):639–652.
[67] Beedle AM, Hamid J, Zamponi GW. Inhibition of transiently expressed low- and high-voltage-activated calcium channels by trivalent metal cations. J Membr Biol. 2002;187(3):225–238.
[68] Biagi BA, Enyeart JJ. Gadolinium blocks low- and high-threshold calcium currents in pituitary cells. Am J Physiol Physiol. 1990;259(3):C515–C520.
[69] Obejero-Paz CA, Gray IP, Jones SW. Y^{3+} block demonstrates an intracellular activation gate for the α_{1G} T-type Ca^{2+} channel. J Gen Physiol. 2004;124 (6):631–640.
[70] Tang S, Mikala G, Bahinski A, et al. Molecular localization of ion selectivity sites within the pore of a human L-type cardiac calcium channel. J Biol Chem. 1993;268:13026–13029.
[71] Ellinor PT, Yang J, Sather WA, et al. Ca^{2+} channel selectivity at a single locus for high-affinity Ca^{2+} interactions. Neuron. 1995;15(5):1121–1132.
[72] Cibulsky SM, Sather WA. The EEEE locus is the sole high-affinity Ca(2+) binding structure in the pore of a voltage-gated Ca(2+) channel: block by Ca(2+) entering from the intracellular pore entrance. J Gen Physiol. 2000;116(3):349–362.
[73] Neumaier F, Dibué-Adjei M, Hescheler J, et al. Voltage-gated calcium channels: determinants of channel function and modulation by inorganic cations. Prog Neurobiol. 2015;129:1–36.
[74] Tang L, Gamal El-Din TM, Payandeh J, et al. Structural basis for Ca^{2+} selectivity of a voltage-gated calcium channel. Nature. 2014;505(7481):56–61.
[75] Shaya D, Findeisen F, Abderemane-Ali F, et al. Structure of a prokaryotic sodium channel pore reveals essential gating elements and an outer ion binding site common to eukaryotic channels. J Mol Biol. 2014;426(2):467–483.

[76] Bourinet E, Zamponi GW, Stea A, et al. The α_{1E} Calcium Channel Exhibits Permeation Properties Similar to Low-Voltage-Activated Calcium Channels. J Neurosci. 1996;16(16):4983–4993.
[77] Cens T, Rousset M, Kajava A, et al. Molecular determinant for specific Ca/Ba selectivity profiles of low and high threshold Ca^{2+} channels. J Gen Physiol. 2007;130(4):415–425.
[78] Feng Z-P, Hamid J, Doering C, et al. Amino acid residues outside of the pore region contribute to N-type calcium channel permeation. J Biol Chem. 2001;276(8):5726–5730.
[79] Sun H-S, Hui K, Lee DWK, et al. Zn^{2+} sensitivity of high- and low-voltage activated calcium channels. Biophys J. 2007;93(4):1175–1183.
[80] Grabsch H, Pereverzev A, Weiergräber M, et al. Immunohistochemical detection of α1E Voltage-gated Ca2+ channel isoforms in cerebellum, INS-1 cells, and neuroendocrine cells of the digestive system. J Histochem Cytochem. 1999;47(8):981–994.
[81] Soong TW, Stea A, Hodson CD, et al. Structure and functional expression of a member of the low voltage-activated calcium channel family. Science. 1993;260 (5111):1133–1136.
[82] Pereverzev A, Vajna R, Pfitzer G, et al. Reduction of insulin secretion in the insulinoma cell line INS-1 by overexpression of a $Ca_v2.3$ (α_{1E}) calcium channel antisense cassette. Eur J Endocrinol. 2002;146:881–889.
[83] Vajna R, Schramm M, Pereverzev A, et al. New isoform of the neuronal Ca^{2+} channel alpha1E subunit in islets of Langerhans and kidney - Distribution of voltage-gated Ca^{2+} channel alpha1 subunits in cell lines and tissues. Eur J Biochem. 1998;257(1):274–285.
[84] Galetin T, Tevoufouet EE, Sandmeyer J, et al. Pharmacoresistant $Ca_v2.3$ (E-type/R-type) voltage-gated calcium channels influence heart rate dynamics and may contribute to cardiac impulse conduction. Cell Biochem Funct. 2013;31(5):434–449.
[85] Cohen R, Buttke DE, Asano A, et al. Lipid modulation of calcium flux through $Ca_v2.3$ regulates acrosome exocytosis and fertilization. Dev Cell. 2014;28 (3):310–321.
[86] Wennemuth G, Westenbroek RE, Xu T, et al. CaV 2.2 and CaV 2.3 (N- and R-type) Ca2+ channels in depolarization-evoked entry of Ca2+ into mouse sperm. J Biol Chem. 2000;275(28):21210–21217.
[87] Saegusa H, Kurihara T, Zong S, et al. Altered pain responses in mice lacking alpha 1E subunit of the voltage-dependent Ca^{2+} channel. Proc Natl Acad Sci. 2000;97:6132–6137.
[88] Matsuda Y, Saegusa H, Zong S, et al. Mice lacking Ca (v)2.3 (alpha1E) calcium channel exhibit hyperglycemia. Biochem Biophys Res Commun. 2001;289 (4):791–795.
[89] Pereverzev A, Mikhna M, Vajna R, et al. Disturbances in glucose-tolerance, insulin-release, and stress-induced hyperglycemia upon disruption of the $Ca_v2.3$ (α_{1E}) subunit of voltage-gated Ca^{2+} channels. Mol Endocrinol. 2002;16:884–895.
[90] Kubota M, Murakoshi T, Saegusa H, et al. Intact LTP and fear memory but impaired spatial memory in mice lacking $Ca_v2.3$ (α_{1E}) channel. Biochem Biophys Res Commun. 2001;282(1):242–248.
[91] Weiergräber M, Henry M, Südkamp M, et al. Ablation of $Ca_v2.3$ / E-type voltage-gated calcium channel results in cardiac arrhythmia and altered autonomic control within the murine cardiovascular system. Basic Res Cardiol. 2005;100(1):1–13.
[92] Lee S-C, Choi S, Lee T, et al. Molecular basis of R-type calcium channels in central amygdala neurons of the mouse. Proc Natl Acad Sci U S A. 2002;99(5):3276–3281.
[93] Weiergräber M, Henry M, Radhakrishnan K, et al. Hippocampal seizure resistance and reduced neuronal excitotoxicity in mice lacking the $Ca_v2.3$ E/R-Type voltage-gated calcium channel. J Neurophysiol. 2007;97(5):3660–3669.
[94] Dibué-Adjei M, Kamp MA, Alpdogan S, et al. $Ca_v2.3$ (R-Type) calcium channels are critical for mediating anticonvulsive and neuroprotective properties of lamotrigine ***In vivo***. Cell Physiol Biochem. 2017;44 (3):935–947.
[95] Sochivko D, Pereverzev A, Smyth N, et al. The $Ca_V2.3$ Ca2+ channel subunit contributes to R-Type Ca2+ currents in murine hippocampal and neocortical neurones. J Physiol. 2002;542(3):699–710.
[96] Weiergräber M, Kamp MA, Radhakrishnan K, et al. The $Ca_v2.3$ voltage-gated calcium channel in epileptogenesis—Shedding new light on an enigmatic channel. Neurosci Biobehav Rev. 2006;30(8):1122–1144.
[97] Day NC, Shaw PJ, McCormack AL, et al. Distribution of α1A, α1B and α1E voltage-dependent calcium channel subunits in the human hippocampus and parahippocampal gyrus. Neuroscience. 1996;71 (4):1013–1024.
[98] Yokoyama CT, Westenbroek RE, Hell JW, et al. Biochemical properties and subcellular distribution of the neuronal class E calcium channel alpha 1 subunit. J Neurosci. 1995;15(10):6419–6432.
[99] Bloodgood BL, Sabatini BL. Nonlinear regulation of unitary synaptic signals by $Ca_v2.3$ voltage-sensitive calcium channels located in dendritic spines. Neuron. 2007;53:249–260.
[100] Dietrich D, Kirschstein T, Kukley M, et al. Functional specialization of presynaptic $Ca_v2.3$ Ca^{2+} channels. Neuron. 2003;39(3):1–20.
[101] Gasparini S, Kasyanov AM, Pietrobon D, et al. Presynaptic R-type calcium channels contribute to fast excitatory synaptic transmission in the rat hippocampus. J Neurosci. 2001;21(22):8715–8721.
[102] Yasuda R, Sabatini BL, Svoboda K. Plasticity of calcium channels in dendritic spines. Nat Neurosci. 2003;6(9):948–955.
[103] Christie BR, Eliot LS, Ito K-I, et al. Different Ca^{2+} channels in soma and dendrites of hippocampal

pyramidal neurons mediate spike-induced Ca^{2+} influx. J Neurophysiol. 1995;73(6):2553–2557.
[104] Kavalali ET, Zhuo M, Bito H, et al. Dendritic Ca^{2+} channels characterized by recordings from isolated hippocampal dendritic segments. Neuron. 1997;18 (4):651–663.
[105] Magee JC, Carruth M. Dendritic voltage-gated ion channels regulate the action potential firing mode of hippocampal CA1 pyramidal neurons. J Neurophysiol. 1999;82(4):1895–1901.
[106] Magee JC, Johnston D. Characterization of single voltage-gated Na^+ and Ca^{2+} channels in apical dendrites of rat CA1 pyramidal neurons. J Physiol. 1995;487(1):67–90.
[107] Siapich SA, Banat M, Albanna W, et al. Antagonists of ionotropic γ-aminobutyric acid receptors impair the $NiCl_2$-mediated stimulation of the electroretinogram b-wave amplitude from the isolated superfused vertebrate retina. Acta Ophthalmol. 2009;87(8):854–865.
[108] Weiergräber M, Henry M, Krieger A, et al. Altered seizure susceptibility in mice lacking the $Ca_v2.3$ E-type Ca^{2+} channel. Epilepsia. 2006;47(5):839–850.
[109] Hainsworth AH, McNaughton NCL, Pereverzev A, et al. Actions of sipatrigine, 202W92 and lamotrigine on R-type and T-type Ca^{2+} channel currents. Eur J Pharmacol. 2003;467(1–3):77–80.
[110] Kuzmiski JB, Barr W, Zamponi GW, et al. Topiramate inhibits the initiation of plateau potentials in CA1 neurons by depressing R-type calcium channels. Epilepsia. 2005;46(4):481–489.
[111] Carvill GL. Calcium channel dysfunction in epilepsy: Gain of CACNA1E. Epilepsy Curr. 2019;19(3):199–201.
[112] Helbig KL, Lauerer RJ, Bahr JC, et al. De Novo pathogenic variants in CACNA1E cause developmental and epileptic encephalopathy with contractures, macrocephaly, and dyskinesias. Am J Hum Genet. 2018;103 (5):666–678.
[113] Pereverzev A, Salehi A, Mikhna M, et al. The ablation of the $Ca_v2.3$/E-type voltage-gated Ca^{2+} channel causes a mild phenotype despite an altered glucose induced glucagon response in isolated islets of Langerhans. Eur J Pharmacol. 2005;511(1):65–72.
[114] Jing X, Li D-Q, Olofsson CS, et al. $Ca_v2.3$ calcium channels control second-phase insulin release. J Clin Invest. 2005;115(1):146–154.
[115] Zhang Q, Bengtsson M, Partridge C, et al. R-type Ca(2+) -channel-evoked CICR regulates glucose-induced somatostatin secretion. Nat Cell Biol. 2007;9(4):453–460.
[116] Mehrke G, Pereverzev A, Grabsch H, et al. Receptor-mediated modulation of recombinant neuronal class E calcium channels. FEBS Lett. 1997;408(3):261–270.
[117] Mergler S, Singh V, Grötzinger C, et al. Characterization of voltage operated R-type Ca^{2+} channels in modulating somatostatin receptor subtype 2- and 3-dependent inhibition of insulin secretion from INS-1 cells. Cell Signal. 2008;20(12):2286–2295.
[118] Banarer S, McGregor VP, Cryer PE. Intraislet hyperinsulinemia prevents the glucagon response to hypoglycemia despite an intact autonomic response. Diabetes. 2002;51(4):958–965.
[119] Maruyama H, Hisatomi A, Orci L, et al. Insulin within islets is a physiologic glucagon release inhibitor. J Clin Invest. 1984;74(6):2296–2299.
[120] Göpel S, Zhang Q, Eliasson L, et al. Capacitance measurements of exocytosis in mouse pancreatic α-, β- and δ-cells within intact islets of Langerhans. J Physiol. 2004;556(3):711–726.
[121] López-González I, Torres-Rodríguez P, Sánchez-Carranza O, et al. Membrane hyperpolarization during human sperm capacitation. MHR Basic Sci Reprod Med. 2014;20(7):619–629.
[122] Baro Graf C, Ritagliati C, Stival C, et al. Determination of a robust assay for human sperm membrane potential analysis. Front Cell Dev Biol. 2019;7:101.
[123] Bailey JL. Factors regulating sperm capacitation. Syst Biol Reprod Med. 2010;56:334–348.
[124] Ho HC, Suarez SS. Hyperactivation of mammalian spermatozoa: function and regulation. Reproduction. 2001;519–526. DOI:10.1530/rep.0.1220519
[125] Sakata Y, Saegusa H, Zong S, et al. Cav 2.3 (α1E) Ca2+ channel participates in the control of sperm function. FEBS Lett. 2002;516(1–3):229–233.
[126] Li Y, Hough CJ, Suh SW, et al. Rapid translocation of Zn^{2+} from presynaptic terminals into postsynaptic hippocampal neurons after physiological stimulation. J Neurophysiol. 2001;86(5):2597–2604.
[127] Frederickson CJ, Hernandez MD, Goik SA, et al. Loss of zinc staining from hippocampal mossy fibers during kainic acid induced seizures: A histofluorescence study. Brain Res. 1988;446(2):383–386.
[128] Kim BJ, Kim YH, Kim S, et al. Zinc as a paracrine effector in pancreatic islet cell death. Diabetes. 2000;49(3):367–372.
[129] Park S-J, Min S-H, Kang H-W, et al. Differential zinc permeation and blockade of L-type Ca^{2+} channel isoforms $Ca_v1.2$ and $Ca_v1.3$. Biochim Biophys Acta - Biomembr. 2015;1848(10):2092–2100.
[130] Anastassov IA, Ripps H, Chappell RL. Cytoprotection by endogenous zinc in the vertebrate retina. J Neurochem. 2014;129(2):249–255.
[131] Anastassov IA. Neuromodulatory and cytoprotective roles of zinc in the vertebrate retina [dissertation]. New York (NY): City University of New York; 2013.
[132] Charton G, Rovira C, Ben-Ari Y, et al. Spontaneous and evoked release of endogenous Zn^{2+} in the hippocampal mossy fiber zone of the rat *in situ*. Exp Brain Res. 1985;58(1):202-205.
[133] Frederickson CJ, Giblin LJ, Krezel A, et al. Concentrations of extracellular free zinc (pZn)e in the central nervous system during simple anesthetization, ischemia and reperfusion. Exp Neurol. 2006;198 (2):285–293.

[134] Vogt K, Mellor J, Tong G, et al. The actions of synaptically released zinc at hippocampal mossy fiber synapses. Neuron. 2000;26(1):187–196.
[135] Erreger K, Traynelis SF. Allosteric interaction between zinc and glutamate binding domains on NR2A causes desensitization of NMDA receptors. J Physiol. 2005;569(2):381–393.
[136] Vergnano AM, Rebola N, Savtchenko LP, et al. Zinc dynamics and action at excitatory synapses. Neuron. 2014;82(5):1101–1114.
[137] Anikstejn L, Charton G, Ben-Ari Y. Selective release of endogenous zinc from the hippocampal mossy fibers *in situ*. Brain Res. 1987;404(1–2):58–64.
[138] Quinta-Ferreira ME, Sampaio Dos Aidos FDS, Matias CM, et al. Modelling zinc changes at the hippocampal mossy fiber synaptic cleft. J Comput Neurosci. 2016;41:323–337.
[139] Assaf SY, Chung S-H. Release of endogenous Zn^{2+} from brain tissue during activity. Nature. 1984;308(5961):734–736.
[140] Besser L, Chorin E, Sekler I, et al. Synaptically released zinc triggers metabotropic signaling via a zinc-sensing receptor in the hippocampus. J Neurosci. 2009;29(9):2890–2901.
[141] Howell GA, Welch MG, Frederickson CJ. Stimulation-induced uptake and release of zinc in hippocampal slices. Nature. 1984;308(5961):736–738.
[142] Kodirov SA, Takizawa S, Joseph J, et al. Synaptically released zinc gates long-term potentiation in fear conditioning pathways. Proc Natl Acad Sci. 2006;103(41):15218–15223.
[143] Qian J, Noebels JL. Visualization of transmitter release with zinc fluorescence detection at the mouse hippocampal mossy fibre synapse. J Physiol. 2005;566(3):747–758.
[144] Qian J, Noebels JL. Exocytosis of vesicular zinc reveals persistent depression of neurotransmitter release during metabotropic glutamate receptor long-term depression at the hippocampal CA3-CA1 synapse. J Neurosci. 2006;26(22):6089–6095.
[145] Ueno S, Tsukamoto M, Hirano T, et al. Mossy fiber Zn^{2+} spillover modulates heterosynaptic N-methyl-D-aspartate receptor activity in hippocampal CA3 circuits. J Cell Biol. 2002;158(2):215–220.
[146] Komatsu K, Kikuchi K, Kojima H, et al. Selective zinc sensor molecules with various affinities for Zn2+, revealing dynamics and regional distribution of synaptically released Zn2+ in hippocampal slices. J Am Chem Soc. 2005;127(29):10197–10204.
[147] Suh SW, Danscher G, Jensen MS, et al. Release of synaptic zinc is substantially depressed by conventional brain slice preparations. Brain Res. 2000;879(1–2):7–12.
[148] Pan E, Zhang X-A, Huang Z, et al. Vesicular zinc promotes presynaptic and inhibits postsynaptic long term potentiation of mossy fiber-CA3 synapse. Neuron. 2011;71(6):1116–1126.
[149] Breustedt J, Vogt KE, Miller RJ, et al. Alpha1E-containing Ca^{2+} channels are involved in synaptic plasticity. Proc Natl Acad Sci U S A. 2003;100(21):12450–12455.
[150] Aiba I, Carlson AP, Sheline CT, et al. Synaptic release and extracellular actions of Zn2+ limit propagation of spreading depression and related events in vitro and in vivo. J Neurophysiol. 2012;107(3):1032–1041.
[151] Williamson A, Spencer D. Zinc reduces dentate granule cell hyperexcitability in epileptic humans. Neuroreport. 1995;6(11):1562–1564.
[152] Takeda A, Hirate M, Tamano H, et al. Susceptibility to kainate-induced seizures under dietary zinc deficiency. J Neurochem. 2003;85(6):1575–1580.
[153] Takeda A, Tamano H, Nagayoshi A, et al. Increase in hippocampal cell death after treatment with kainate in zinc deficiency. Neurochem Int. 2005;47(8):539–544.
[154] Blasco-Ibáñez JM, Poza-Aznar J, Crespo C, et al. Chelation of synaptic zinc induces overexcitation in the hilar mossy cells of the rat hippocampus. Neurosci Lett. 2004;355(1–2):101–104.
[155] Domínguez MI, Blasco-Ibáñez JM, Crespo C, et al. Zinc chelation during non-lesioning overexcitation results in neuronal death in the mouse hippocampus. Neuroscience. 2003;116(3):791–806.
[156] Traboulsie A, Chemin J, Chevalier M, et al. Subunit-specific modulation of T-type calcium channels by zinc. J Physiol. 2007;578(1):159–171.
[157] Kang H-W, Vitko I, Lee -S-S, et al. Structural determinants of the high affinity extracellular zinc binding site on Ca_v 3.2 T-type calcium channels. J Biol Chem. 2010;285(5):3271–3281.
[158] Paoletti P, Ascher P, Neyton J. High-affinity zinc inhibition of NMDA NR1-NR2A receptors. J Neurosci. 1997;17(15):5711–5725.
[159] Gingrich KJ, Burkat PM. Zn^{2+} inhibition of recombinant GABAA receptors: an allosteric, state-dependent mechanism determined by the γ-subunit. J Physiol. 1998;506(1–2):609–625.
[160] Emdin SO, Dodson GG, Cutfield JM, et al. Role of zinc in insulin biosynthesis. Some possible zinc-insulin interactions in the pancreatic β-cell. Diabetologia. 1980;19(3):174–182.
[161] Li YV. Zinc and insulin in pancreatic beta-cells. Endocrine. 2014;45(2):178–189.
[162] Robertson RP, Zhou H, Slucca M. A role for zinc in pancreatic islet β-cell cross-talk with the α-cell during hypoglycaemia. Diabetes Obes Metab. 2011;13:106–111.
[163] Franklin I, Gromada J, Gjinovci A, et al. Beta-cell secretory products activate alpha-cell ATP-dependent potassium channels to inhibit glucagon release. Diabetes. 2005;54(6):1808–1815.
[164] Gyulkhandanyan AV, Lu H, Lee SC, et al. Investigation of transport mechanisms and regulation of intracellular Zn^{2+} in pancreatic α-cells. J Biol Chem. 2008;283(15):10184–10197.

[165] Zhou H, Zhang T, Harmon JS, et al. Zinc, not insulin, regulates the rat alpha-cell response to hypoglycemia *in vivo*. Diabetes. 2007;56:1107–1112.
[166] Ramracheya R, Ward C, Shigeto M, et al. Membrane potential-dependent inactivation of voltage-gated ion channels in alpha-cells inhibits glucagon secretion from human islets. Diabetes. 2010;59(9):2198–2208.
[167] Ravier MA, Rutter GA. Glucose or insulin, but not zinc ions, inhibit glucagon secretion from mouse pancreatic alpha-cells. Diabetes. 2005;54(6):1789–1797.
[168] Göpel SO, Kanno T, Barg S, et al. Regulation of glucagon release in mouse α-cells by KATP channels and inactivation of TTX-sensitive Na+ channels. J Physiol. 2000;528(3):509–520.
[169] Gromada J, Ma X, Hoy M, et al. ATP-sensitive K^+ channel-dependent regulation of glucagon release and electrical activity by glucose in wild-type and SUR1-/- mouse-cells. Diabetes. 2004;53(Supplement 3):S181–S189.
[170] Holmkvist J, Tojjar D, Almgren P, et al. Polymorphisms in the gene encoding the voltage-dependent Ca^{2+} channel $Ca_v2.3$ (CACNA1E) are associated with type 2 diabetes and impaired insulin secretion. Diabetologia. 2007;50(12):2467–2475.
[171] Muller YL, Hanson RL, Zimmerman C, et al. Variants in the $Ca_v2.3$ (α_{1E}) subunit of voltage-activated Ca^{2+} channels are associated with insulin resistance and type 2 diabetes in Pima Indians. Diabetes. 2007;56(12):3089–3094.
[172] Trombetta M, Bonetti S, Boselli M, et al. CACNA1E variants affect beta cell function in patients with newly diagnosed type 2 diabetes. The verona newly diagnosed type 2 diabetes study (VNDS) 3. PLoS One. 2012;7(3):e32755.
[173] Tietz NW, Logan NM. Textbook of clinical chemistry (Appendix). Tietz NW, editor. Philadelphia: Saunders; 1986.
[174] Bremner I, May PM. Systemic interactions of zinc. In: Mills CF, editor. Zinc Hum Biol. New York: Springer Verlag; 1989. p. 95–108.
[175] Reyes JG. Zinc transport in mammalian cells. Am J Physiol Physiol. 1996;270(2):C401–C410.
[176] Kerns K, Zigo M, Sutovsky P. Zinc: a necessary ion for mammalian sperm fertilization competency. Int J Mol Sci. 2018;19(12):4097.
[177] Setchell BP, Maddocks S, Brooks DE, et al. Anatomy, vasculature, innervation and fluids of the male reproductive tract. In: Knobil E, Neill JD, Ewing LLeditors. Physiol Reprod. New York: Raven; 1988. p. 753–835.
[178] Kim AM, Bernhardt ML, Kong BY, et al. Zinc sparks are triggered by fertilization and facilitate cell cycle resumption in mammalian eggs. ACS Chem Biol. 2011;6(7):716–723.
[179] Que EL, Duncan FE, Bayer AR, et al. Zinc sparks induce physiochemical changes in the egg zona pellucida that prevent polyspermy. Integr Biol. 2017;9(2):135–144.